electron-nuclear spin interaction does not exist. A very small chemical shift for band B is consistent with a Li_2 molecule model. This model is also consistent with a Lorenzian line shape. The intermolecular force between two Li_2 molecules is based on a weak van der Waals bond, and Li_2 molecules can move rather freely. Therefore, the magnetic effect caused by surrounding nuclei is averaged in the same way as in a liquid phase. In a liquid phase, the NMR line shape is determined by the relaxation through spin-spin interaction. The observed half width for band B is not much narrower than that of band A. We suppose that there is a very efficient spin-spin relaxation process in a Li_2 molecule mediated by bonding electrons. Site B may be called a "covalent" site.

The extra specific capacity of PPP-based carbon can be interpreted to result from the presence of the "covalent" site B. The capacity of site A may be restricted by the GIC stoichiometry, whereas the capacity of site B may have no limit opposed by the electronic system stability because occupation of site B involves little change in the electronic state of the carbon host. Only a geometrical limit exists for the B site capacity. The most saturated state may be C_2Li, where each benzene ring of PPP-based carbon is accompanied by one Li atom.

The charge-discharge mechanism of the lithium ion in PPP-based carbon can be understood as follows (Fig. 3). The Li ions in site A form a $\sqrt{3} \times \sqrt{3}$ commensurate lattice structure, which is the reason for the stoichiometric restriction of site A, similar to that in the well-known Li GIC (*1*). A Li_2 molecule in covalent site B is loosely trapped upon two adjacent benzene rings, which are not occupied by site A Li ions. The bond length of Li_2 is 2.672 Å (9), which is slightly longer than the distance between the centers of two adjacent hexagonal rings (2.46 Å). Therefore, Fig. 3 is not a geometrically unacceptable image. The distance between two nearest neighbor Li atoms in metallic Li is 3.032 Å. Only a covalent character in the Li-Li bond can make the occupation of site B possible. In the charging process, site B is occupied at first, and then, after the charged capacity has exceeded 300 A·hour/kg, site A occupation begins. In the discharging process, Li ions in ionic A sites are released at first. When a vacancy on site A is created, it is reoccupied through dissociation and charge transfer reaction of Li_2 molecules on B sites. The Li_2 molecules in B sites are able to act as a capacity reservoir.

Assuming that each benzene ring of PPP-based carbon can supply one site for Li occupation, the calculated specific capacities per weight and per volume are 1157 A·hour/kg and 2983 A·hour/liter, respectively. Those for Li metal are 3862 A·hour/kg and 2061 A·/liter, respectively. These high specific capacities suggest the possibility of a high-energy battery that is more compact when made with Li ions (or molecules) than when made with Li metal.

Recently, Conard *et al.* (*10*) synthesized highly saturated Li GIC (C_2Li, 1116 A·hour/kg) from highly oriented pyrolytic graphite under high pressure (50 to 60 kbar). The PPP-based carbon can store almost the same amount of Li under ambient pressure and temperature by an electrochemical reaction on a nanometer length scale in disordered carbons. This phenomenon may provide a promising breakthrough and future for high-energy Li batteries to be used for various applications.

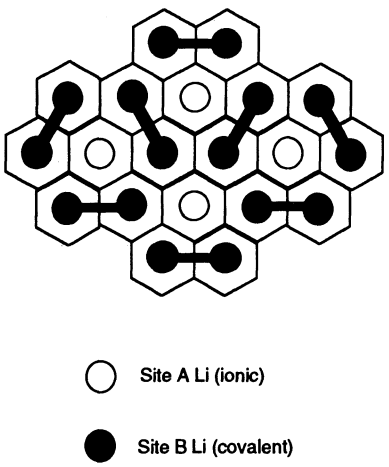

Fig. 3. Schematic illustration for the coexistence of two types of Li site in PPP-based carbon. Reduced aromatic rings are represented by hexagonals. The Li ions and atoms are denoted by empty and solid circles for sites A and B, respectively. Covalent bonds between two Li atoms in site B are shown by heavy lines.

REFERENCES AND NOTES

1. M. S. Dresselhaus and G. Dresselhaus, *Adv. Phys.* **30**, 139 (1981).
2. T. Nagaura and T. Tozawa, *Prog. Batteries Sol. Cells* **9**, 209 (1990).
3. M. Noguchi, K. Miyashita, M. Endo, *Tanso* **155**, 315 (1992).
4. S. Yata *et al.*, in *Proceedings of the 60th Conference of the Electrochemical Society of Japan*, T. Nonaka, Ed. (Electrochemical Society of Japan, Tokyo, 1993), p. 184.
5. P. Kovacic and A. Kyriakis, *J. Am. Chem. Soc.* **85**, 454 (1963).
6. K. Oshida *et al.*, *J. Mater. Res.* **8**, 512 (1993).
7. D. Guerard and A. Herold, *Carbon* **13**, 337 (1975).
8. A. Abragam, *The Principles of Nuclear Magnetism* (Oxford Univ. Press, Oxford, 1961), pp. 191–210.
9. F. W. Loomis and R. E. Nusbaum, *Phys. Rev.* **38**, 1447 (1931).
10. J. Conard, V. A. Nalimova, D. Guerard, in *Extended Abstracts of the 7th International Symposium on Intercalation Compounds*, J. P. Issi, Ed. (Organizing Committee of ISIC7, Louvain–La Neuve, 1993), p. 114.

3 November 1993; accepted 1 March 1994

A Putative Role of the Xanthophyll, Zeaxanthin, in Blue Light Photoreception of Corn Coleoptiles

Miguel A. Quiñones* and Eduardo Zeiger†

Both flavins and carotenoids have some of the attributes expected for a photoreceptor mediating blue light–induced phototropism in plants. Besides the classical photoreceptor candidate, β-carotene, coleoptiles contain many other carotenoids, including the main components of the xanthophyll cycle, violaxanthin and zeaxanthin. Here, dark-grown coleoptiles accumulated violaxanthin, but lacked zeaxanthin. Coleoptiles devoid of zeaxanthin did not bend in response to a blue light pulse. Coleoptile tips converted violaxanthin into zeaxanthin in the light. Manipulation of coleoptile zeaxanthin content by red light, red light plus darkness, or incubation with the inhibitor of zeaxanthin formation, dithiothreitol, resulted in a blue light–induced bending that was proportional to zeaxanthin content. These data indicate that zeaxanthin may be a blue light photoreceptor in corn coleoptiles.

The identity of the photoreceptor for blue light–induced phototropism (*1*) remains unknown. Available action spectra (*2*) implicate both flavins and carotenoids, and a plasma membrane–bound flavoprotein is currently hypothesized as the most likely chromophore (*3*). On the other hand, chloroplasts may be a site of photoreception for phototropism in oat coleoptiles (*4*), and guard cell chloroplasts show a blue light response that has an action spectrum matching the absorption spectrum of carotenoids (*5*). Here, we investigated whether the carotenoid, zeaxanthin, which has an absorption spectrum matching the action spectrum for phototropism (*2*), could mediate blue light–induced phototropic bending. In chloroplasts from higher plants, violaxanthin is converted to zeaxanthin in the light by way of an intermediate, antheraxanthin (*6*). Zeaxanthin reverts to violaxanthin

Department of Biology, University of California at Los Angeles, Los Angeles, CA 90024, USA.

*Present address: Centro de Investigaciones Biológicas–Consejo Superior de Investigaciones Cientificas, Velázquez 144, Madrid-28006, Spain.
†To whom correspondence should be addressed.

in the dark. The zeaxanthin produced by this xanthophyll cycle functions in the photoprotection of the photosynthetic apparatus (*7*). If zeaxanthin also mediates blue light photoreception, then coleoptile chloroplasts should operate the xanthophyll cycle, and the blue light–induced phototropic response should be quantitatively related to zeaxanthin concentrations in the tissue.

We tested whether corn coleoptile cells operate the xanthophyll cycle. Coleoptiles were grown in the dark (*8*) for 3 days. Coleoptile tips (1.5 mm) were harvested and their pigment content was analyzed by high-performance liquid chromatography (HPLC) (*9*). Dark-grown coleoptiles had no zeaxanthin, little antheraxanthin, and high violaxanthin concentrations (Fig. 1A, inset). Coleoptile tips kept in an oxygenated solution and illuminated with white light accumulated zeaxanthin (Fig. 1A) and showed a concomitant decrease in violaxanthin, implicating a functional xanthophyll cycle in their chloroplasts. Red and blue light also stimulated zeaxanthin accumulation and a decrease in violaxanthin (*10*). Thus, like white light in mesophyll chloroplasts (*7*), blue and red light modulate chloroplast processes that result in zeaxanthin accumulation.

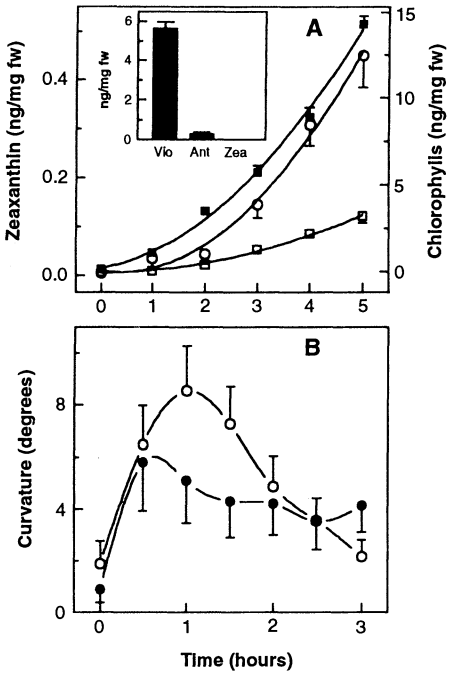

Fig. 1. (**A**) Accumulation of zeaxanthin and chlorophylls in dark-grown coleoptiles exposed to white light (1250 μmol m^{-2} s^{-1}). Zeaxanthin (○), chlorophyll *a* (■), and chlorophyll *b* (□). (**Inset**) Xanthophyll content in dark-grown coleoptiles. Vio, violaxanthin; Ant, antheraxanthin; Zea, zeaxanthin. (**B**) Kinetics of the phototropic response induced by a blue light pulse (1 μmol m^{-2} s^{-1}, 200 s) on dark-grown corn coleoptiles preilluminated with red light (500 μmol m^{-2} s^{-1}) for 1.5 hours (●) or 3 hours (○). Values are the average of three experiments ± SD.

Chloroplasts abound in epidermal cells from light-grown coleoptiles. The chloroplasts stream inside thin cytoplasmic strands appressed between the plasma membrane and the tonoplast and fluoresce in red when viewed under fluorescence microscopy. On illumination with white light, dark-grown coleoptile tips also accumulate chlorophylls *a* and *b* (Fig. 1A), suggesting that the chlorophyll-xanthophyll protein complexes found in mesophyll chloroplasts (*11*) are also assembled in coleoptile chloroplasts during greening. Isolated corn coleoptile chloroplasts operate the xanthophyll cycle and accumulate zeaxanthin in white light (*12*). These findings indicate that coleoptile chloroplasts are functional.

We used red light treatments (*13*) of different durations to vary the zeaxanthin content of coleoptiles, in order to study the relation between zeaxanthin content and responsiveness to blue light. Zeaxanthin accumulation was maximal, about 0.6 ng/mg fresh weight, after a 3.5-hour irradiation with red light (Fig. 2A). Intermediate times of irradiation resulted in intermediate amounts of zeaxanthin accumulation. Dark-adapted, light-grown coleoptiles irradiated with white light accumulated maximal zeaxanthin in less than 30 min (*12*), suggesting that the time course of zeaxanthin formation in dark-grown coleoptiles (Fig. 2A) is lengthened by the greening process. Maximal zeaxanthin levels in 5-day-old corn leaves comprised about 40% of the total xanthophyll pool, compared with 25% in light-grown coleoptiles (*12*) and about 10% in dark-grown ones (Fig. 2A).

The blue light sensitivity of coleoptiles containing different zeaxanthin concentrations was assayed by measurement of maximum curvature in response to a unilateral blue light pulse (*14*). A part of each coleoptile batch was harvested for pigment analysis by HPLC immediately after the pulse. The rest was kept in the dark and used for curvature measurements. Responses to subsaturating blue light pulses of both guard cells and coleoptiles are proportional to pulse fluence (*15, 16*). Therefore, use of a weak actinic pulse made it possible to correlate zeaxanthin content at the time of the pulse with maximum curvatures measured 40 to 60 min later.

The phototropic response to the blue light pulse was transient, and the coleoptiles resumed vertical growth after some time (Fig. 1B). As reported previously (*17*), longer light pretreatments induced greater curvatures. Because the length of the light pretreatment altered the time at which maximum curvature was reached, curvatures were measured every 10 min in order to determine maximum curvature for each treatment.

Zeaxanthin content and maximum curvature were closely related (Fig. 2A). Coleoptiles with no detectable zeaxanthin were insensitive to a blue light pulse (*18*), and coleoptiles with maximal zeaxanthin levels had the largest phototropic response. Intermediate zeaxanthin concentrations were highly correlated with attained curvatures (Fig. 2A, inset). The enhancement of blue light–induced phototropism by red light pretreatments has usually been interpreted as a phytochrome-mediated response (*16, 19*). The close correspondence between bending and the red light–dependent zeaxanthin content indicates that the response to red light pretreatments could also be mediated by zeaxanthin.

Zeaxanthin concentrations were also varied by exposure to darkness after the 3.5-hour

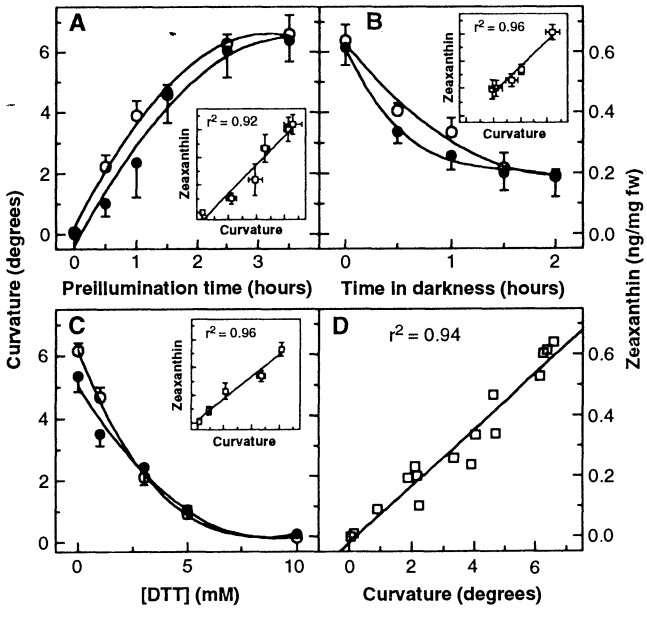

Fig. 2. (A to C) Effects of the duration of red light pretreatment (**A**), length of exposure to darkness (**B**), or exposure to different DTT concentrations (**C**) on the blue light–induced phototropic response (○) and the zeaxanthin content (●) of dark-grown corn coleoptiles. Coleoptiles were illuminated with red light for 3.5 hours before being placed in darkness (B) or after being sprayed with DTT (C). (**D**) Correlation between the magnitude of the blue light–induced phototropic response and the zeaxanthin content of corn coleoptiles in all treatments. Insets of (A), (B), and (C) show the correlation for each treatment, including error bars for all values. Results are the average of five experiments ± SD.

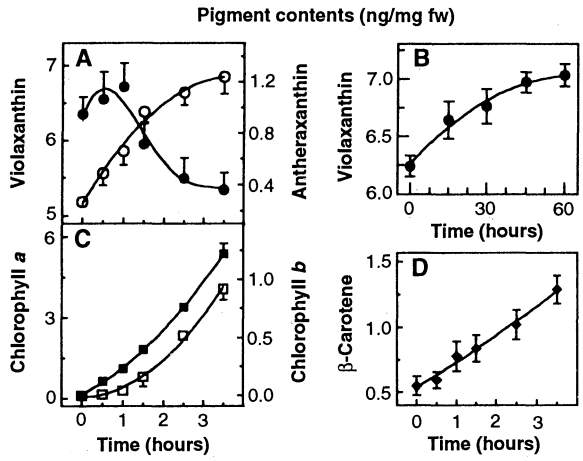

Fig. 3. Effect of the duration of red light pretreatment on the pigment content of dark-grown coleoptiles (**A** to **D**). Violaxanthin (●), antheraxanthin (○), chlorophyll *a* (■), chlorophyll *b* (□), and β-carotene (◆). Values are the average of five experiments ± SD. (B) Violaxanthin content in dark-grown coleoptiles during the first hour of illumination with red light. Values are the average of three experiments ± SD. Other conditions were as described in Fig. 2.

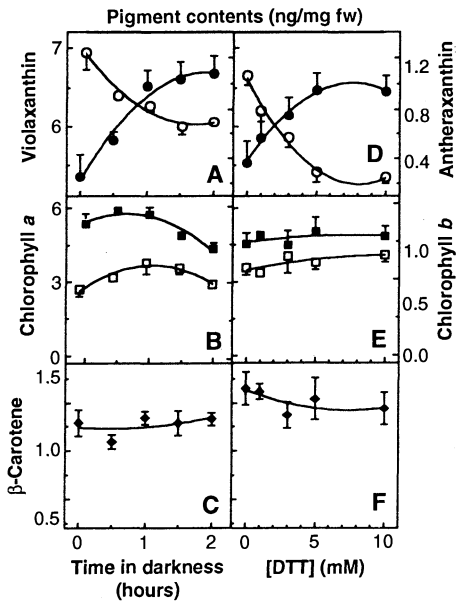

Fig. 4. Changes in pigment content of dark-grown corn coleoptiles as a function of time in the dark, after a 3.5-hour red light pretreatment (**A** to **C**) or exposure to different DTT concentrations followed by a 3.5-hour red light pretreatment (**D** to **F**). Violaxanthin (●), antheraxanthin (○), chlorophyll *a* (■), chlorophyll *b* (□), and β-carotene (◆). Values are the average of five experiments ± SD. Other conditions were as described in Figs. 2 and 3.

treatment with red light. As in mesophyll tissue (*20*), zeaxanthin content was greatest at the end of the red light period and declined as a function of time in the dark (Fig. 2B). In contrast with dark-grown coleoptiles, however, light-treated coleoptiles had measurable zeaxanthin levels after exposures to darkness of up to several hours. The blue light sensitivity of the preilluminated, dark-treated coleoptiles declined in parallel with their zeaxanthin content (Fig. 2B), and the two parameters were highly correlated (Fig. 2B, inset).

Coleoptile zeaxanthin content could also be varied by exposure to increasing concentrations of the inhibitor of violaxanthin deepoxidation, dithiothreitol (DTT) (*21*). Coleoptiles sprayed with 10 mM DTT and subsequently exposed to red light lacked detectable zeaxanthin and failed to bend in response to blue light (Fig. 2C). Intermediate DTT concentrations resulted in intermediate zeaxanthin contents and curvatures. At all DTT concentrations, the magnitude of the phototropic response to blue light was positively correlated with zeaxanthin content (Fig. 2C, inset). The results obtained in the presence and absence of DTT (Fig. 2, A to C) argue against the possibility that the relation between bending and zeaxanthin concentrations is coincidental and that the elicited light responses are mediated by an unidentified photoreceptor. Irrespective of the treatment used to elicit changes in zeaxanthin concentration, the relation between zeaxanthin content at the time of the pulse and the magnitude of the blue light–induced phototropic response was the same in all treatments (Fig. 2D).

In contrast, with the exception of antheraxanthin, none of the other pigments analyzed covaried with blue light sensitivity (Figs. 3 and 4). Chlorophylls and β-carotene increased with the duration of the red light treatment but, unlike zeaxanthin, their increase did not saturate after 3.5 hours of irradiation (Fig. 3, C and D) and their content did not change significantly in darkness or DTT-treated coleoptiles (Fig. 4, B, C, E, and F). Antheraxanthin changed in parallel with zeaxanthin (Figs. 3A and 4, A and D), but the results showing that dark-grown coleoptiles had antheraxanthin (Fig. 1A) but did not respond to a blue light pulse (Fig. 2B) argue against a role of antheraxanthin in blue light photoreception.

Concentrations of violaxanthin, the precursor to zeaxanthin, changed in the opposite direction to those of zeaxanthin (Figs. 3A and 4, A and D). Hence, the blue light sensitivity of the coleoptile could be associated with a promoting role of zeaxanthin or an inhibitory role of violaxanthin. However, measurements made at 15-min intervals showed a net increase in violaxanthin during the first hour of the red light pretreatment (Fig. 3B), which paralleled the zeaxanthin increase. An inhibitory role of violaxanthin in photoreception is thus inconsistent with the relation between the blue light sensitivity of the coleoptiles and their violaxanthin content.

We thus show a quantitative relation between the concentration of a putative chromophore and the blue light sensitivity of the tissue. Besides its absorption spectrum, zeaxanthin has other attributes predicted for a blue light photoreceptor: (i) it is present in low concentrations (*22*), (ii) it is the photoproduct of a cyclic reaction that regenerates its precursor in the dark (*15, 16*), and (iii) its concentration in red light–treated tissue increases in parallel with blue light sensitivity. Blue light photoreception by zeaxanthin in the coleoptile chloroplast could stimulate a cascade of events, which might include electrogenic proton pumping (*23*), leading to asymmetric growth and bending.

REFERENCES AND NOTES

1. L. S. Kaufman, *Plant Physiol.* **102**, 333 (1993).
2. W. Shropshire Jr. and R. B. Withrow, *ibid.* **33**, 360 (1958).
3. T. W. Short, M. Ports, W. R. Briggs, *Photochem. Photobiol.* **55**, 773 (1992); K. M. F. Warpeha, L. S. Kaufman, W. R. Briggs, *ibid.*, p. 595.
4. H. P. Sorokin and K. V. Thimann, *Nature* **187**, 1038 (1960).
5. A. Srivastava and E. Zeiger, *Plant Physiol.* **100**, 1562 (1992); M. A. Quiñones and E. Zeiger, in preparation.
6. H. Y. Yamamoto, *Pure Appl. Chem.* **51**, 639 (1979).
7. B. Demmig-Adams, *Biochim. Biophys. Acta* **1020**, 1 (1990); W. Bilger and O. Björkman, *Photosynth. Res.* **25**, 173 (1990).
8. Corn seeds (*Zea mays* L., Pioneer hybrid 3362) were soaked in tap water for 24 hours and planted between two layers of garden soil in metal or plastic trays. Trays were placed in the dark at 30°C and 90% humidity and watered daily.
9. For the pigment extraction, 35 coleoptile tips (previously weighed) were homogenized in acetone (0.5 ml, $NaHCO_3$ saturated) plus hexane (2 ml, $NaHCO_3$ saturated) for 2 min. KCl (0.5 ml, 0.2 M) was added and the mixture centrifuged at 5000 rpm for 3 min. The upper phase was collected and evaporated under vacuum. The dry extracts were flushed with nitrogen and stored at −80°C. All solvents used were ice-cold and the extraction was performed under dim room light. We separated chlorophylls and carotenoids in a Beckman HPLC system provided with an Altech Spherisorb ODS-1 column using the method described by A. M. Gilmore and H. Y. Yamamoto [*J. Chromat.* **543**, 137 (1991)].
10. Excised coleoptile tips were treated as described above for the experiments with white light. Red and blue lights were obtained from slide projectors provided with a Schott RG-6 (Duryea, PA) red filter or an Ealing (South Natick, MA) blue filter (450 nm, broad band). Fluence rates used were 250 and 500 μmol m^{-2} s^{-1} for both types of radiation.
11. J. P. Thornber, *Encycl. Plant Physiol.* **19**, 98 (1986).
12. J. Zhu and E. Zeiger, unpublished results.
13. Red light of 500 μmol m^{-2} s^{-1} was supplied to the coleoptiles from above with the use of a ProDesign Network LED array (Santa Clara, CA) with peak emission at 660 nm.
14. Trays with dark-grown coleoptiles (either pre-

treated with red light or not) were placed, one at a time, in front of a Dolan-Jenner Fiber Illuminator (Woburn, MA) provided with an Ealing blue filter used to induce phototropic curvature. On one side of the tray (90° from the blue light beam), a TV camera (Javelin Electronics, Torrance, CA) was placed. This camera was connected to a personal computer equipped with a Jandel Video Analysis Software (Corte Madera, CA). Images were saved every 10 min after the blue light pulse (1 μmol m^{-2} s^{-1} for 200 s), in which at least 25 coleoptiles were identified and their curvature at the tip was measured. All experiments were conducted in a dark room, and whenever light was necessary to obtain a clear image of the coleoptiles, a low-intensity green light source, having no overlap with the blue light spectrum, was used.
15. M. Iino, T. Ogawa, E. Zeiger, *Proc. Natl. Acad. Sci. U.S.A.* **82**, 8019 (1985).
16. M. Iino, *Planta* **171**, 110 (1987).
17. G. M. Curry, thesis, Harvard University (1957); W. R. Briggs and H. P. Chon, *Plant Physiol.* **41**, 1159 (1966).
18. In contrast with the effect of long, continuous exposures to actinic blue light commonly used to measure fluence response curves [R. Viestra and K. Poff, *Plant Physiol.* **68**, 798 (1981)], weak actinic pulses prevented stimulation of zeaxanthin formation by blue light and minimized phytochrome-mediated phototropic responses [M. Iino, W. R. Briggs, E. Schäfer, *Planta* **60**, 41 (1984); J. C. Young, E. Liscum, R. P. Hangarter, *ibid.* **188**, 106 (1992)]. Either response would have precluded characterization of treatments resulting in the absence of a specific blue light response.
19. H. P. Chon and W. R. Briggs, *Plant Physiol.* **41**, 1715 (1966).
20. B. Demmig, K. Winter, A. Krüger, F.-C. Czygan, *ibid.* **84**, 218 (1987).
21. Dark-grown coleoptiles were sprayed with different DTT solutions (0, 1, 3, 5, and 10 mM) 3 hours and 1 hour before being exposed to red light for 3.5 hours.
22. W. R. Briggs, in *Photophysiology*, A. Geise, Ed. (Academic Press, London, 1964), vol. 1, pp. 223–271.
23. E. E. Serrano, E. Zeiger, S. Hagiwara, *Proc. Natl. Acad. Sci. U.S.A.* **85**, 436 (1988).
24. We thank R. Bogomolni, D. Chapman, O. Björkman, H. Yamamoto, L. Talbott, and M. Iino for generous insight on spectroscopy, carotenoid biochemistry, xanthophyll physiology and biochemistry, and HPLC and pulse methodology; A. Levi and D. Adler for work on initial DTT experiments; and L. Talbott and L. Kaufman for comments on the manuscript. M.A.Q. gratefully acknowledges a Fulbright fellowship. Supported by NSF grant MCB 93-06801.

17 November 1993; accepted 9 March 1994

The Role of Interleukin-6 in Mucosal IgA Antibody Responses in Vivo

Alistair J. Ramsay,* Alan J. Husband, Ian A. Ramshaw, Shisan Bao, Klaus I. Matthaei, Georges Koehler, Manfred Kopf

In mice with targeted disruption of the gene that encodes interleukin-6 (IL-6), greatly reduced numbers of immunoglobulin A (IgA)–producing cells were observed at mucosae and grossly deficient local antibody responses were recorded after mucosal challenge with either ovalbumin or vaccinia virus. The IgA response in the lungs was completely restored after intranasal infection with recombinant vaccinia viruses engineered to express IL-6. These findings demonstrate a critical role for IL-6 in vivo in the development of local IgA antibody responses and illustrate the effectiveness of vector-directed cytokine gene therapy.

Immune responses at mucosal surfaces are characterized by production and secretion of antibodies of the IgA isotype, which represent a first line of defense against colonization by many pathogens (*1*). Most IgA antibody-containing cells (ACCs) originate in mucosa-associated lymphoid tissue (MALT), such as Peyer's patches in the intestine, where they encounter antigen. Subsequently, ACCs disseminate by means of draining lymph and blood circulation to mucosal effector sites where IgA production occurs (*1, 2*). Efforts to design effective mucosal vaccines, given impetus by the current human immunodeficiency virus (HIV) epidemic (*3*), have been hampered by a lack of information regarding mucosal immunoregulation. Although the induction of mucosal IgA responses is known to be dependent on cognate help provided by $CD4^+$ T cells in MALT (*4*), factors important in the subsequent development of these responses have not been well defined. Interleukin-6, a multifunctional cytokine originally identified for its ability to induce B cell terminal differentiation (*5, 6*), markedly and selectively enhances IgA production in vitro by isotype-committed B cells (*7, 8*). The in vivo relevance of these findings has not been determined, but the presence in mucosal tissues of T cells, macrophages, and other cells capable of IL-6 production in vitro (*1, 8, 9*), and the broad distribution of cells containing IL-6 mRNA in intestinal mucosa (*10*), are consistent with the proposition that this factor is important in regulating the effector stage of IgA responses.

To obtain evidence for this hypothesis, we studied mucosal IgA antibody responses in mice rendered deficient in IL-6 production ($IL\text{-}6^-$) by targeted disruption of the gene that encodes IL-6 (*11*). These mice develop normally but fail to mount optimal responses to injury or infection. In particular, although amounts of total serum immunoglobulin are similar in $IL\text{-}6^-$ mutants and their normal ($IL\text{-}6^+$) littermates, the mutants have impaired serum IgG antibody responses to virus infection (*11*). These mice provide an ideal opportunity for assessment of the in vivo relevance of IL-6 to mucosal IgA responses (*12*). We addressed this question by determining the difference in total and antigen-specific IgA plasma cell distribution and IgA antibody production in the intestines and lungs of $IL\text{-}6^-$ and $IL\text{-}6^+$ mice immunized with protein antigen or infected with recombinant vaccinia virus (rVV).

In the absence of deliberate immunization, mutant mice had substantially fewer IgA plasma cells in their small intestines, mesenteric lymph nodes (MLN), and lungs compared to $IL\text{-}6^+$ mice (Figs. 1A and 2, A and B). In addition, IgA-positive cells stained much less intensely in the mutants. Increased numbers of IgM-positive cells were found in mutants (Fig. 1A), especially in MLN, possibly reflecting a block in the differentiation pathway toward IgA production. The paucity of IgA plasma cells in $IL\text{-}6^-$ mice was consistent with the distribution of IL-6 mRNA in intestines as determined by in situ hybridization; whereas IL-6 mRNA was broadly distributed throughout the lamina propria of $IL\text{-}6^+$ mice (Fig. 2C), no such signal was detected in $IL\text{-}6^-$ mice (Fig. 2D). The residual number of IgA plasma cells in the latter may arise from a minor subset of IgA precursor cells, which come from the peritoneal cavity rather than MALT (*13*) and which appear to develop independently of IL-6 (*14*).

We next determined the consequences of IL-6 deficiency on the development of mucosal antibody responses. The capacity of mutant mice to mount specific intestinal IgA ACC responses after local immunization with ovalbumin was grossly deficient (Fig. 1B). To study responses to virus infection, we immunized mice intranasally with rVV constructs (*15*) encoding the gene for the hemagglutinin (HA) glycoprotein of influenza virus, with or without the murine IL-6 gene (VV-HA-IL-6 or VV-HA-TK, respectively), and monitored their production of HA antibody and the number of HA-specific antibody-secreting cells (ASCs) in the lungs. Recombinant VV constructs encoding genes for foreign proteins produce these factors in a highly localized manner at sites and in amounts determined by the extent of virus replica-

A. J. Ramsay, I. A. Ramshaw, K. I. Matthaei, The John Curtin School of Medical Research, Australian National University, Canberra 0200, Australia.
A. J. Husband and S. Bao, Department of Veterinary Pathology, University of Sydney, Sydney NSW 2006, Australia.
G. Koehler and M. Kopf, Max Planck Institute for Immunobiology, Stuebeweg 51, D-79108 Freiburg, Germany.

*To whom correspondence should be addressed.